Astron. Astrophys. 323, 739–748 (1997)

ASTRONOMY AND ASTROPHYSICS

Radio-loud active galaxies in the northern ROSAT All-Sky Survey

II. Multi-frequency properties of unidentified sources⋆

W. Brinkmann[1], J. Siebert[1], E.D. Feigelson[2], R.I. Kollgaard[2], S.A. Laurent-Muehleisen[2], W. Reich[3], E. Fürst[3], P. Reich[3], W. Voges[1], J. Trümper[1], and R. McMahon[4]

[1] Max-Planck-Institut für Extraterrestrische Physik, Giessenbachstrasse, D-85740 Garching, Germany
[2] Dept. of Astronomy & Astrophysics, The Pennsylvania State University, University Park, PA 16802, USA
[3] Max-Planck-Institut für Radioastronomie, Auf dem Hügel 69, D-53121 Bonn, Germany
[4] Institute of Astronomy, Madingley Road, Cambridge CB3 OHA, UK

Received 6 August 1996 / Accepted 14 January 1997

Abstract. We present the broad band, radio - to - X-ray, properties of a large sample of mostly previously optically unidentified radio-loud X-ray sources from the correlation of a ROSAT All-Sky Survey source list with the 5 GHz Green Bank Survey of the northern sky (RGB sample) which is one of the largest well-defined flux-limited surveys of AGN ever obtained. Further, the RGB pushes 1-2 orders of magnitude deeper in both X-ray and radio flux compared to previous unbiased wide-area AGN surveys.

Follow up VLA observations of the candidate objects yielded positions with arcsec accuracy which were used to find optical counterparts to the sources from digitized POSS plates. The sources are divided into three classes according to the positional offset between the X-ray and radio candidates and the spatial resolution of the radio observations, reflecting the various degrees of confidence about the correctness of the proposed association.

Although the nature of the sources as well as their redshifts remain to be determined in spectroscopic follow up observations, the derived flux ratios lead to the conclusion that the majority of them are quasars. Hardly any correlations could be found between different source parameters, possibly due to the fact that most of the objects are found in a relatively small flux range near the sensitivity limit of the radio catalogue.

The majority of the new RGB sources have broad-band properties between those of traditional radio-selected and X-ray selected AGN. There is no bimodal distribution in the radio-loudness distribution, and the traditional division between radio-quiet and radio-loud AGN may not be warranted

Key words: galaxies: active – quasars; X-rays: general – radio sources: general

Send offprint requests to: W. Brinkmann

⋆ Tables 1-4 are available in electronic form at the CDS via anonymous ftp 130.79.128.5

1. Introduction

The ROSAT All-Sky Survey was the first soft X-ray survey of the whole sky using an imaging telescope (Trümper 1983) with a limiting sensitivity of a few $\times 10^{-13}$ erg cm^{-2} s^{-1}. The cross - correlation of the ROSAT All-Sky Survey source list (Voges 1992) with existing radio catalogues yielded a comprehensive sample of radio-loud extragalactic X-ray sources with unprecedented low flux limits of the radio and X-ray catalogues. In a previous paper (Brinkmann et al. 1995, B95) we presented the results of a cross - correlation of the ROSAT All-Sky Survey source list with a source list generated from the Condon et al. (1989) 5 GHz survey of the northern sky (RGB = RASS - Green Bank sources). From the 2127 coincidences, only 617 sources had been previously optically identified as extragalactic objects. From now on we will refer to these sources as being 'known'; the other objects are called 'unknown'.

A first sample of 234 radio sources has been studied in follow up observations with the 100-m Effelsberg telescope to obtain more accurate positions and contemporaneously measured radio spectra between 21 cm and 2.8 cm (Neumann et al. 1994). Subsequently, multi-frequency Effelsberg observations have been carried out for a large number of more than 510 sources stronger than 100 mJy at 5 GHz. The results of these observations are given in an accompanying paper (Reich et al. in prep.).

All sources have further been studied in snapshot mode with the VLA in various configurations (Laurent-Muehleisen et al. 1997, L97) to obtain arcsec positions and 5 GHz core fluxes. With these accurate positions we were able to find plausible optical counterparts for most of the sources from digitized POSS plates (McMahon 1991).

In this paper we will present a discussion of the broad band bulk properties of the objects. Although the actual nature of the objects can only be determined by optical spectroscopy, the fluxes and colours in the different wave bands provide sufficient information for an approximate classification and allow a

comparative study of these objects with the previously known sources. Further, it has recently become obvious (c.f. B95) that any analysis based on objects with existing classifications only is bound to be biased towards sources with extreme properties in at least one of the observing bands, mostly towards those with high fluxes. For example, nearly all of the strong radio sources of the 1 Jy sample (Kühr et al. 1979) have been optically identified and many of them have been studied at other wavelengths as well (Stickel & Kühr 1996). Therefore, phase space diagrams constructed to understand the broad band characteristics of various radio-loud AGN classes are usually restricted to regions of high radio fluxes. The current sample with much lower limiting sensitivities in all wavelength bands than any previous surveys, and with a nearly uniform coverage of a large part of the sky, can certainly shift these boundaries into unexplored regions.

The outline of the paper is as follows. In the next section we will give an overview over the contents and the properties of the used catalogues, the selection criteria, and we will present the source catalogue with the relevant X-ray, optical, and radio information. In Sect. 3 we will discuss the general radio to X-ray properties of the objects and we will compare the results to those obtained for the previously known objects in the sample and other studies.

2. The X-ray - radio content of the sample

The ROSAT All-Sky Survey was performed from August 1, 1990 to February 1, 1991 and yielded $\sim$ 50000 X-ray sources with a positional accuracy such that 68% of the sources are found within $20''$ from their corresponding optical counterparts, and a limiting sensitivity of a few times 10^{-13} erg cm^{-2} s^{-1}in the 0.1 - 2.4 keV energy band depending on the spectral form and the amount of Galactic absorption. For details of the survey and first results see Voges (1992).

The data were processed by a quasi - automatic Standard Analysis Software System (SASS, Voges et al. 1992). The currently used source list is expected to be complete to $\sim$ 90%. This incompleteness arises from a geometrical effect caused by the SASS processing of the data in 2^o strips in ecliptical coordinates. Towards the strip boundaries the source detection algorithm becomes insensitive and the detection efficiency drops, a software problem which was overcome in the more recent RASS-II processing. We further have to remark that the obtained results may depend slightly on the current parameter settings of the SASS and thus might be marginally different after the reprocessing of the data.

The radio survey that covers most of the northern sky $0^o \leq \delta_{1950} \leq +75^o$ at highest sensitivity is that conducted by Condon et al. (1989) at 6 cm wavelength with the Green Bank 300 ft telescope. The angular resolution of the survey is about $3\farcm7 \times 3\farcm3$ and the noise in the maps has been measured to be about 5 mJy/beam area, but increases below 30° declination up to about 8 mJy/beam area at 0° declination. From the survey maps a catalogue of $\approx$ 150000 small diameter sources at a flux density level above 15 mJy was prepared (for details see Neumann et al. 1994). The majority of them is rather faint: more than 10^5 sources have fluxes $\leq$ 50 mJy. The positional accuracy varies from $10''$ for stronger sources to about $30''$ for weak sources in each coordinate.

We looked for correlations between the radio and the X-ray positions with angular separations of less than $100''$ and found a total of 2127 sources. The cumulative distribution of the separations between the X-ray and radio positions is well represented by a Gaussian with $\sigma \sim 17''$ for angular separations up to $\approx$ $40''$ (see Fig. 1 in B95). This radius thus includes more than about 98% of the true coincidences while at larger separations, due to the large number of sources in both catalogues, the rate of chance coincidences is not negligibly small, an effect which is noticed in the follow up VLA observations. However, for the stronger radio objects the absolute number of erroneous coincidences is rather low: for sources with radio fluxes $\gtrsim$ 50 mJy we expect $\sim$ 48 chance coincidences for angular separations $\leq 60''$ and $\sim$ 135 for separations up to $100''$ out of the 2127 sources, so the sample reliability would be about 98% or 94%, respectively (B95).

The number of X-ray - radio correlations found in a certain radio flux interval appears to be subject to a strong selection effect caused by the limiting sensitivity of the X-ray survey. The detection probability rises from about 1% at the lowest radio flux levels to $\sim$ 20% of the sources with a flux $\geq$ 2 Jy (see Fig. 2 of B95). We probably see changes in the typical source population as well: at low radio fluxes the fraction of galaxies compared to the number of quasars is higher than at high radio fluxes. However, X-ray detection biases and selection effects in the optical identification of the sources also influence the sample composition.

By making use of the NASA/IPAC Extragalactic Data Base (NED) and recent ROSAT related optical identification programs, we were able to identify 617 objects and to study their class specific multi- frequency properties (B95). It was found that known and unknown objects were clearly discriminated by a selection effect as, apart from some exceptions, the unknown sources were found at the lower end of the radio flux scale. The reason is that large scale surveys with high sensitivity became available only recently and it further indicates that previous attempts for an optical identification of radio sources have been biased by their apparent strength, i.e., the brightest sources were identified first.

To obtain accurate source positions and core radio fluxes, all objects were observed with the VLA in snap shot mode. The details and the results of these observations are presented by Laurent-Muehleisen et al. (1997) (L97). For 1861 radio sources sub-arcsec positions and fluxes could be obtained, 436 sources were observed only at low resolution and in 72 fields no source was found with a signal-to-noise greater than 5 (see Sect. 2.1).

For all VLA sources we determined plausible optical counterparts from O and E POSS plates digitized with the Automatic Plate Measuring (APM) machine at $1.0''$ resolution (McMahon 1991). Usually, there is an optical object at angular distances less than a few arcsec from the VLA position, but for a small number of sources the closest optical object is more than $20''$

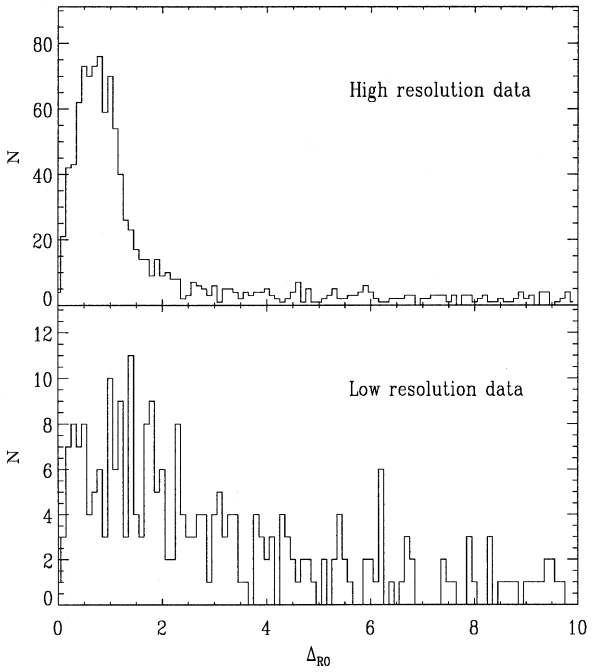

Fig. 1. Distribution of VLA - optical positions for the high resolution (upper panel) and low resolution (lower panel) radio data in arcsec.

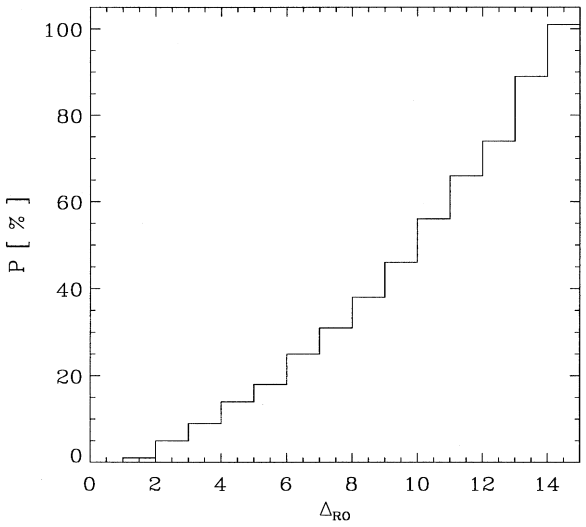

Fig. 2. Probability P in % to find an optical object by chance with an angular separation $< \Delta_{RO}$ from a random position.

away. Usually, this indicates a chance coincidence but in in some cases the radio sources are extended or multiple.

In Fig. 1 we show the distribution of distances (in arcsec) between the VLA positions and the nearest optical counterparts. In the high resolution data 86% of the objects have distances $\leq 4''$, for the low resolution data (D configuration) about 75% of the objects are found at distances less than $4''$.

A rigorous analysis of the reliability and completeness of the current sample is certainly highly desired. However, an analysis relying on the positional coincidence of the objects in the different wavelength bands only, for example with a Likelihood Ratio analysis as done for flux limited radio - optical surveys (Windhorst et al. 1984) seems to be insufficient for a quantitative assessment as we are dealing with a 'pre selected' sample (via the radio - X-ray correlations). The X-ray selection is spatially and spectrally inhomogeneous and depends in a presently not well understood way on the classes of the sources. Secondly, it has been argued recently (Wall 1996, Wagner 1996) that a positional coincidence of the objects in different wavelength bands is not always a sufficient criterion for the physical association of the sources. To assess the reliability of the coincidences we took a heuristic approach and obtained a lower limit for the number of chance coincidences by looking at a large number of positions offset $5'$ in declination from radio positions and counted the number of cases where the nearest optical candidate was found inside a given angular distance. In Fig. 2 we plot the probability to find an unrelated point-like optical object within a given radius. It reveals that this fraction is $\sim 10\%$ for distances up to $4''$ and inside an angular distance of $15''$ we always find at least one optical object on the plates. For further analyses relying on the optical properties of the counterparts we will thus only take objects with separations of $\Delta \leq 4''$ which appears to be a fair compromise between the number of chance coincidences and completeness of the sample. However, we list all sources and give the angular separation between the radio and the nearest optical object in the tables.

The photometric magnitudes are accurate up to ~ 0.05 mag but there are zero point uncertainties for faint objects below 18 mag in R and systematic errors for bright extended objects (galaxies) which vary from plate to plate. Further, the O-E colours which can be used for a rough characterization of the objects (McMahon, 1991) are quite reliable in the range $-1 \leq O-E \leq 3$, but outside this range non linearity effects start to dominate.

2.1. The data

In Tables 1 - 3 we present the relevant X-ray and optical data for all previously optically unidentified extragalactic ROSAT - 5 GHz GB sources. We present only a sample page of each table here; a full copy of the tables is available from the CDS via anonymous ftp to cdsarc.u-strasbg.fr. The radio data are given in L97; the corresponding data for the 'known' objects can be found in B95. Table 1 contains the objects where the positional offset between X-ray and VLA source is $\leq 40''$, in Table 2 we list the objects with $\Delta_{rx} > 40''$. Table 3 is for the low resolution (D-configuration) data.

Column 1 gives the ROSAT All-Sky Survey identification of the X-ray source, followed by the J2000 position of the VLA source, which is assumed to be the radio counterpart. In some cases, there is more than one VLA object close to the ROSAT position (for the following statistical analyses we always used the closest one). In column 3 the distance in arcsec between the VLA and the X-ray source is given followed by the corrected 5 GHz flux density (from L97). The X-ray flux in the 0.1 - 2.4 keV energy range with its statistical error in units of

10^{-12} erg cm^{-2} s^{-1}(for details see below) is given in column 5, followed by the power law photon index of the X-ray source deduced under the assumption of Galactic absorption. If no values are given the quality of the data does not allow the determination of a meaningful spectral index. Then the E- and O-magnitudes of the optical counterpart are given and a value for the classification of the optical object: 1 for 'non-stellar', -1 for 'star-like', 0 for 'noise-like', 2 for 'possible blend'. On the O-plates about 63% of the $\gtrsim$ 1400 classified sources are 'star-like', 25% are 'non-stellar', and 12% are blends. Only very few objects are 'noise-like'. These ratios are slightly different on the E-plates with more objects classified as 'non-stellar' and 'blend' instead of 'star-like'. Both classifications are, therefore, given in the tables. An entry $'ef'$ in the magnitude column indicates an empty field on the plate, dots that no plate is available. The positional difference (in arcsec) between VLA and optical object is given in column 11. In the next column we note with an asterix if a source has been re-observed with the Effelsberg telescope (Reich et al. in prep.). Finally, we note if an object has been optically classified recently (after publication of B95) and give a key for the corresponding reference. For the classification: i stands for 'object has been identified', q stands for quasar, g for galaxy, and b for BL Lac object.

We obtained the X-ray fluxes from the measured count rates by assuming an average photon index of Γ = 2.2 for the underlying X-ray spectrum and Galactic absorption (Dickey & Lockman 1990, Stark et al. 1992; for details see Brinkmann et al. 1994). The stated errors merely reflect the errors in the counting statistics of the survey sources and do not incorporate deviations from the assumed power law slope, additional absorption, or systematic errors depending on the form of the local X-ray background and on details of the detection algorithm. Therefore, a total error of the X-ray flux of the order of $\lesssim 25\%$ must be regarded as a conservative estimate.

The quoted photon indices were estimated using the two hardness ratios given by the SASS (Voges et al. 1992) applying the method described in Brinkmann et al. (1994), for fixed Galactic absorption. The errors of the power law indices were estimated from the errors of the hardness ratios (Schartel 1995).

It should be noted that in the following scientific analysis of the broad band properties of the sources only objects with an optical - to - radio separation of $\Delta_{ro} \leq 4''$ and with $\Delta_{rx} \leq 40''$ are included.

Finally, in Table 4 we list 72 sources where the VLA observations did not reveal a source. The majority of these objects are very faint in the original 87 GB source list and might just be spurious. The few stronger sources appear to be extended and are mostly located at low Galactic latitudes. Several of them could be identified as Galactic foreground objects like supernova remnants or planetary nebulae.

3. The radio to X-ray properties of the objects

Fig. 3 shows the spatial distribution of the sample in Galactic coordinates. Previously identified objects (B95) and objects for which ID's have been published recently (see the notes in tables 1-3) are indicated by crosses. Circles represent the currently unidentified objects with symbols proportional in size to their X-ray fluxes. Clearly visible are the spatial boundaries of the Green Bank Survey ($0^o \leq \delta \leq 75^o$) and a strip of initially missing Survey exposure, which was filled in later in August 1991, however, with slightly shorter exposure.

3.1. Flux distributions

In Fig. 4 we show the distribution of the objects as function of their fluxes in the different wavelength bands; (top: total 5 GHz flux density (in mJy); middle: optical magnitude, obtained from NED or, if not available, from the POSS plates (m_o if given, otherwise m_E); bottom: soft X-ray flux).

The full line represents all objects of the RGB sample, the shaded areas are the previously known objects. The sharp decline of the number of objects at low radio and X-ray fluxes is a direct consequence of the sensitivity limit of the RASS and the corresponding $log(N) - log(S)$ distribution (Fig. 2 of B95) shows that the X-ray sensitivity is insufficient to detect the radio sources at all flux densities at the same rate. Clearly visible are further the identification biases with respect to the observed fluxes. This effect is particularly strong for the radio fluxes as nearly all sources with fluxes above 1 Jy have been identified previously; i.e., they are contained in the 1 Jy sample (Stickel & Kühr 1996). In the optical band more than half of the unidentified objects are fainter than 18th magnitude (the 325 empty fields on the plates are plotted in the first bin) and in the X-ray range only the very brightest objects show a substantial degree of identification. The figure thus directly reflects previous biases towards stronger sources and demonstrates the importance of sensitive large scale sky surveys for the study and characterization of multi wavelength class properties of the sources.

3.2. X-ray properties

The low background of the PSPC detector allows an approximate determination of the X-ray spectral parameters from a relatively small number of photons. As the average Survey exposure on a source is rather low ($\sim$ 400 s) only for the strongest sources a sufficiently large number of photons could be accumulated for proper spectral fits. For the majority of the sources a hardness ratio method had to be applied in which the hardness ratios, provided by the SASS processing, are mapped onto power law slopes, assuming free or Galactic absorption towards the source (for details of the method see B95). This allows an approximate spectral determination for objects with count rates as low as 0.03 cts/s or even less if the exposure is correspondingly high (for example, at higher ecliptical latitudes). Further, the assumption of Galactic absorption towards the sources leaves one free parameter in the procedure which is then equivalent to a least square fit of the underlying power law slope.

3.2.1. Spectral properties

The results of a maximum-likelihood analysis for the distribution of power law slopes for the unidentified sources and, for

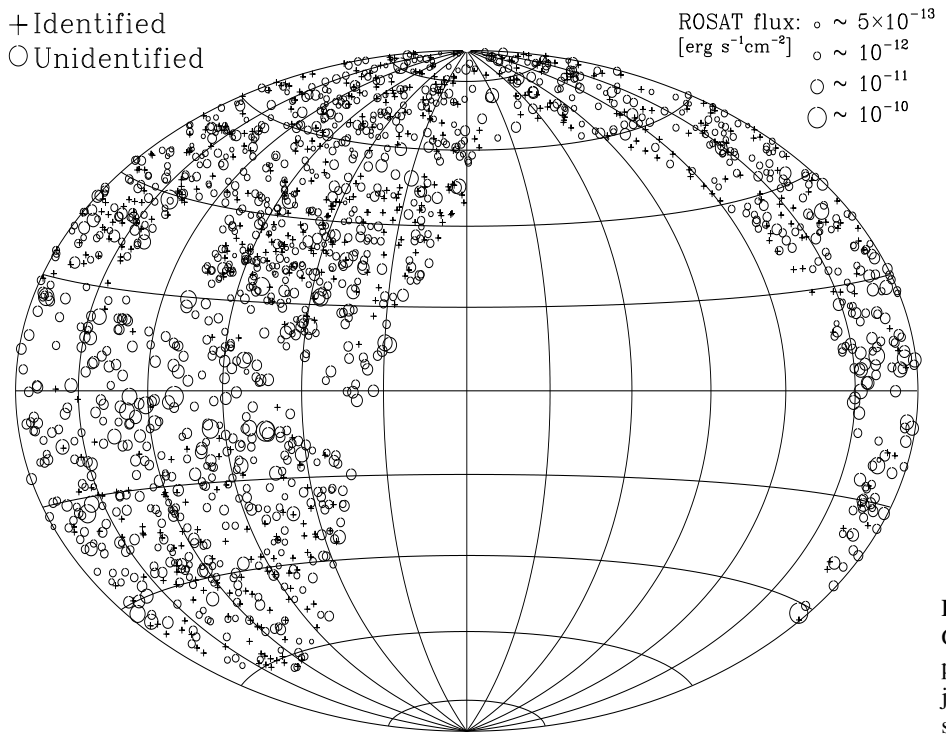

Fig. 3. The RGB AGN sample plotted in Galactic coordinates. The symbol sizes are proportional to the X-ray flux of the objects. Crosses represent optically identified sources.

Table 5.

Object class	$N_{H,galactic}$			$N_{H,free}$		
	N	$\bar{\Gamma} \pm 1\sigma$	σ^{intr}	N	$\bar{\Gamma} \pm 1\sigma$	σ^{intr}
Quasars	197	2.14±0.06	0.22±0.06	165	2.20±0.21	<0.34
Galaxies	115	1.92±0.10	0.47±0.08	101	1.96±0.17	<0.24
Seyferts	41	2.02±0.14	0.46±0.11	37	2.04±0.24	0.45±0.23
BL Lacs	91	2.23±0.06	0.25±0.06	80	2.35±0.11	<0.15
Unidentified	938	2.23±0.04	0.40±0.03	815	2.34±0.11	<0.17

comparison, for the known quasars and galaxies from B95 are given in Table 5 (for details of the analysis see Maccacaro et al. 1988, Worrall & Wilkes 1990). For completeness we list the values for the small group of Seyfert galaxies in the 87 GB sample as well. The spectral indices obtained for fits assuming Galactic N_H are shown in Fig. 5.

The contours correspond to 90% confidence levels. The significant intrinsic dispersion is an indicator for either the inhomogeneity of the sample; i.e., it consists of non-separated subclasses of objects with different spectral properties, or the individual sources show an intrinsically large dispersion of their spectral properties. Spectral curvature, combined with a large redshift range might also contribute to the dispersion. However, due to the limited photon statistics for most of the sources we cannot apply more complex spectral models to the data. In this respect it should be noted that, for fits with free absorption, all classes (apart from Seyfert galaxies, not shown in Fig. 5) have a dispersion compatible with zero.

The rather steep average index of the unknown objects, although comparable to that of the quasars within their mutual errors, nevertheless raises some questions. Its high value does not support the intuitive assumption that the sample consists of a mixture of mainly quasars and radio galaxies. Further, at higher redshifts the quasar spectra flatten considerably (Brinkmann et al. 1996a) so that the faint sources in the current sample cannot be predominantly distant, and therefore faint quasars. As the ROSAT Survey detection rate of known distant radio loud quasars is rather high, all of them with flat X-ray spectra (this holds for pointed observations with ASCA as well, see Cappi et al. 1997), it seems unlikely that we are finding a completely new class of high-z, steep X-ray spectrum quasars. BL Lac objects seem to possess similar steep power law slopes but optical follow up programs for suitably pre-selected sources from our sample (see Sect. 3.4.1) yield a BL Lac identification rate of $\sim$ 30% (Laurent-Muehleisen 1996) with the majority of the studied objects being quasars and radio galaxies. Finally, it should be noted that there seems to be a general hardening of source spectra with decreasing X-ray flux in deep ROSAT observations (Vikhlinin et al. 1995), recently attributed to an increasing contribution of X-ray luminous galaxies (Almaini et al. 1996) which further argues against a strong contribution of these sources in our sample.

In Fig. 6 we show the distribution of the spectral indices of the unknown objects (obtained with Galactic absorption) compared to the (suitably normalized) distribution of power law indices for nearly 600 radio-loud quasars seen by ROSAT (shaded area; from Brinkmann et al. 1996a). Clearly visible is an excess of sources with very steep spectra compared to the quasar distribution. A correlation of these sources with various other observational properties reveals that the steep X-ray spectrum sources are predominantly those with lowest count rates, with higher Galactic N_H - values, and that they are mostly found to-

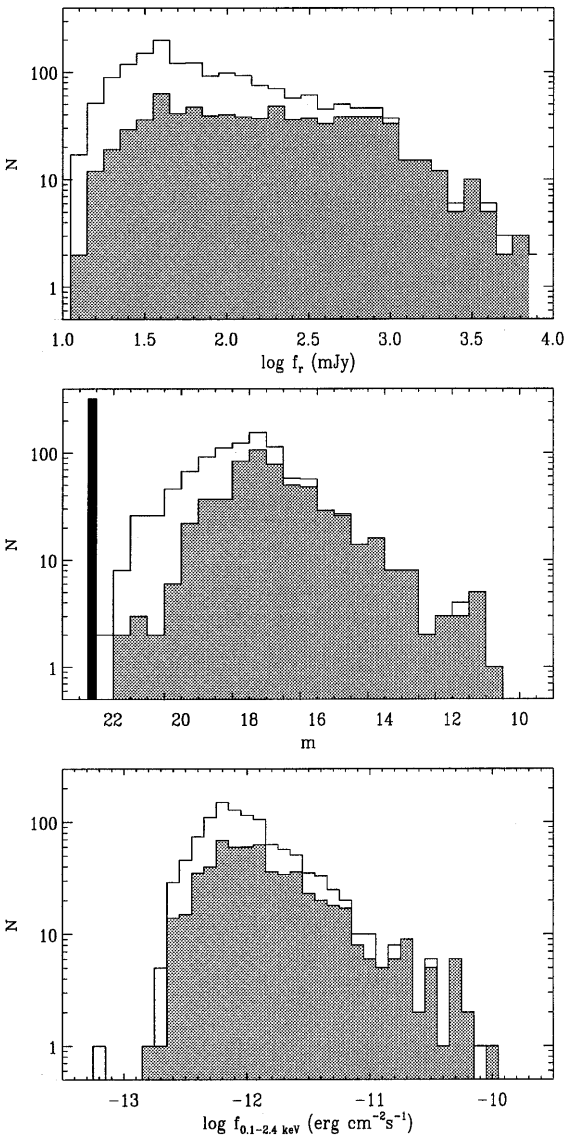

Fig. 4. Number of RGB sources as function of their fluxes in different wavelength bands. From top to bottom: number of objects per radio flux interval, per optical magnitude interval and as function of the soft 0.1 - 2.4 keV X-ray flux. Open histograms denote the distributions of all objects, the shaded areas indicate previously optically identified objects. The first bin in the optical distribution denotes radio objects without optical counterpart on the plates within 4″

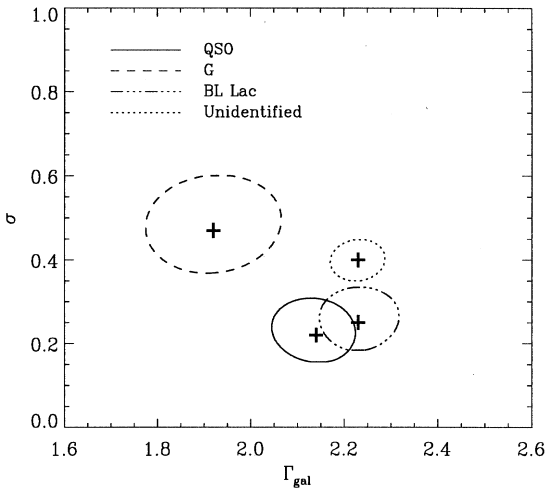

Fig. 5. Best-fit mean spectral index and Gaussian standard deviation for power law fits to different classes of objects in the RGB sample assuming Galactic absorption. Contours correspond to 90% confidence levels.

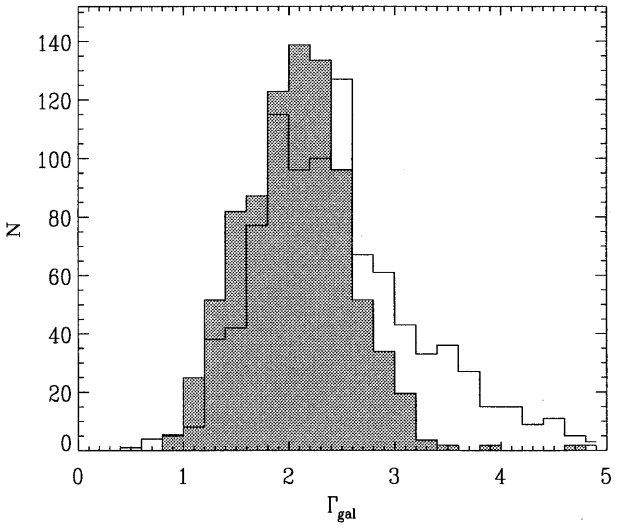

Fig. 6. Histogram of the spectral index distribution of the unknown objects, compared to that of radio-loud quasars (shaded area). In both cases Galactic absorption was assumed.

wards lower Galactic latitudes (see Fig. 7). The latter indicates that a certain fraction of the objects might be mis-identifications in the sense that they are not radio-loud AGN but that the X-ray emitters are more likely Galactic foreground objects, i.e., stars. However, the main effect seems to be the high absorbing column density towards lower Galactic latitudes which, for objects with low count rates, leads to systematic biases in the determination of the hardness ratios in the SASS and thus to apparently steeper spectra. Finally, the low number of counts for many of the the objects further hints at a previously known selection effect, that at the lowest count rates sources with steeper spectral slopes have a slightly higher detection probability.

Finally, it should be noted that in Fig. 6 the known quasars show an excess of flat X-ray spectrum objects ($\Gamma \leq 1.8$) compared to the current sample. For the known quasars this region is populated by Gigahertz Peaked Spectrum (GPS) objects and flat spectrum radio sources at higher redshifts. The deficit of unknown objects in this X-ray power law slope range seems to indicate that the sample does not contain a substantial number of those objects.

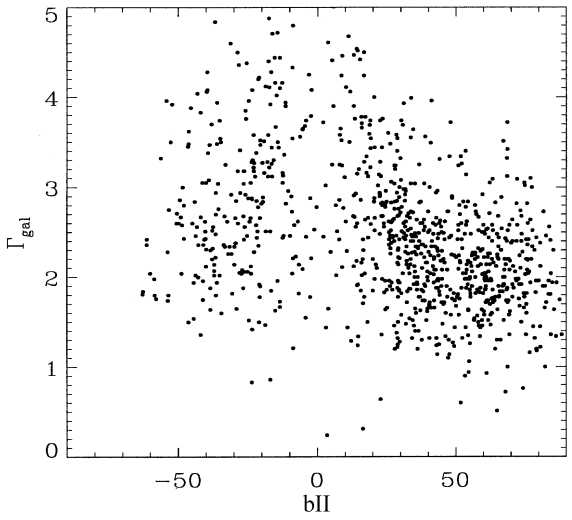

Fig. 7. Photon index Γ as function of Galactic latitude bII.

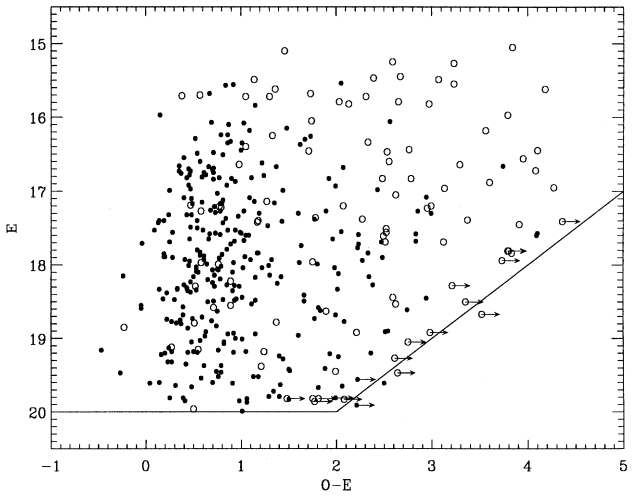

Fig. 8. Red E magnitudes as function of the colour of the optical continuum. • : objects which appear point like on the POSS plates, ○ : objects classified as non stellar. Rightward pointing errors denote the absence of an image on the O plate, i.e., a very red object. The lines indicate the plate limits.

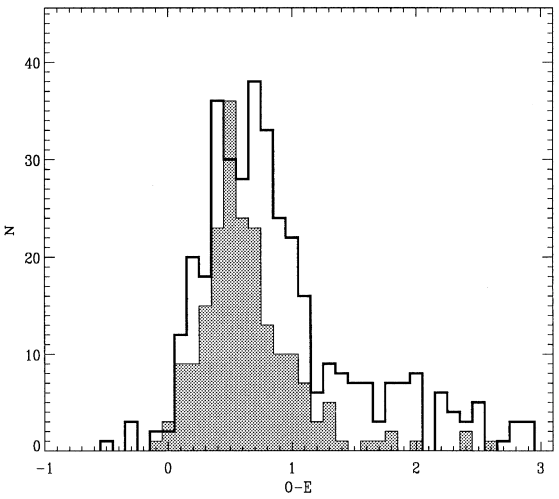

Fig. 9. Histogram of the distribution of the colours O-E of the unknown objects, classified as point like, in comparison to the colours of the known quasars in the sample (hatched area).

3.3. Optical properties

The proposed optical counterparts in Table 1 - 3 were merely selected according to their proximity to the VLA sources. They might not always be, especially in cases of larger positional differences, the 'real' counterparts of the X-ray emitters, although the correspondence between radio source and optical object seems to be established in most cases. For many of the sources which are seen towards the Galactic plane and which are, therefore, more likely chance coincidences with foreground objects, there is no optical information available from the POSS plates and they are not included in our analysis. Thus, we are confident that the majority of the cases for which we can determine optical magnitudes are the correct optical counterparts and the magnitudes and colours can be used for a rough classification.

In Fig. 8 we show the colour - magnitude diagram for the objects for which this information is available. Objects classified as non stellar are generally redder. They should be mostly radio galaxies. Point-like objects with O-E ≤ 0.8 are likely to be quasars as can be seen from the comparison with the colours of known quasars in Fig. 9, and field objects, drawn from the control sample of objects with $5'$ offset positions show a broad peak in the range $1 \leq O - E \leq 2$. Very red point-like objects can either be candidates for 'red quasars', quasars at higher redshifts, or faint distant galaxies (Mc Mahon 1991). However, as mentioned above, for colours redder than O-E ~ 3 nonlinearity effects become important and the exact value of the colour must be treated cautiously.

3.4. Flux ratios

The lack of any redshift and morphological information for the sources excludes luminosity correlations which are currently employed to study the bulk emission properties of different object classes. Flux ratios provide as well nearly distance independent measures of the emission characteristics, only differences in the K-corrections are neglected.

3.4.1. The $\alpha_{ro} - \alpha_{ox}$ diagram

The availability of fluxes from the radio to the X-ray has been extensively used in the past for a classification of extragalactic objects (Tananbaum et al. 1979, Stocke et al. 1991). Based on two-point spectral indices, the radio-to-optical α_{ro} = $log(S_{\nu_{opt}}/S_{\nu_{rad}})/log(\nu_{rad}/\nu_{opt})$ and optical-to-X-ray α_{ox} = $-log(S_{\nu_x}/S_{\nu_{opt}})/log(\nu_x/\nu_{opt})$, it could be shown that different classes of objects typically populate different regions of the $\alpha_{ro} - \alpha_{ox}$ diagram.

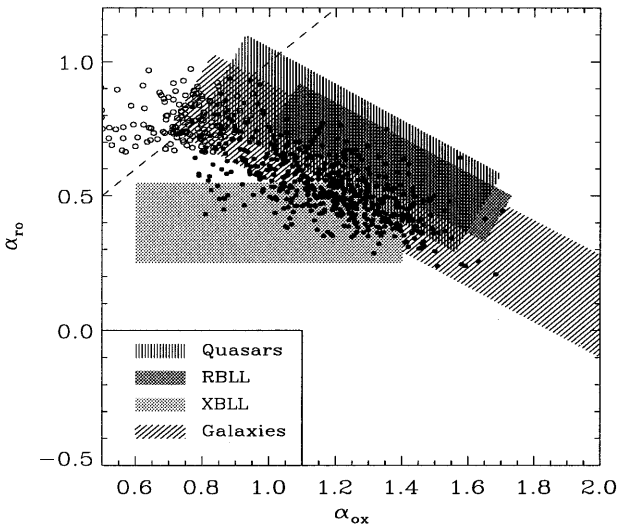

Fig. 10. $\alpha_{ro} - \alpha_{ox}$ diagram constructed from values as given in Tab. 1 - 3. Shaded areas denote typical regions of known object classes. Open circles represent point like objects for which only upper limits can be given for the optical fluxes ($m_O \geq 22$). Objects above the dashed line have an inverted spectral energy distribution (see text).

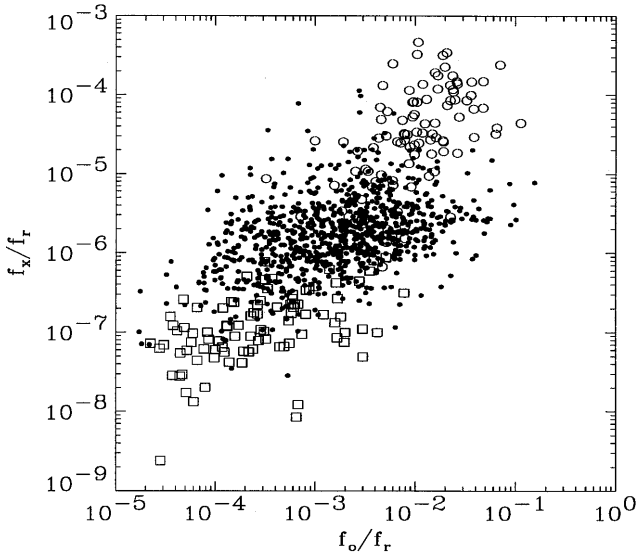

Fig. 11. Logarithmic flux ratios log (f_x/f_r) as function of log (f_o/f_r). Open circles are X-ray selected BL Lacs, open squares radio selected BL Lacs and HPQ (from Brinkmann et al. 1996b); full dots: the current sample.

For the construction of the $\alpha_{ro} - \alpha_{ox}$ diagram, the 5 GHz total flux densities from the Green Bank survey were used; for the monochromatic optical fluxes we took the O-magnitudes from the POSS plates (if available, otherwise the correspondingly corrected E-magnitudes). The monochromatic X-ray fluxes at 2 keV were computed as in B95 using the measured count rates and the PSPC energy-to-counts conversion factor for power law spectra. For the photon indices Γ we took the ensemble average of $< \Gamma > \sim 2.2$ obtained in Sect. 3.2.1. The adoption of this mean value allows us to avoid the large scatter of the spectral indices introduced by the limited photon statistics, although in some cases it may result in an incorrect flux determination if the actual spectral index of a source truly differs from the mean value. In contrast to similar diagrams (B95, Brinkmann et al. 1994) the fluxes are not K-corrected as the types and the redshifts of the objects remain unknown. The shift in phase space expected from the K-corrections for an object at z = 1 and with typical quasar power law slopes (α_r = 0.5, α_o = 0.5, and α_x = 1.2) is, however, rather small: $\Delta\alpha_{ox} \leq 0.1$, while the value of α_{ro} does not change with the above assumed spectral slopes.

The hatched regions represent the typical areas where the different object classes are generally found. The diagram shows that the phase space region at larger α_{ox} values, usually populated by nearby optically bright galaxies with low X-ray and radio emission remains devoid of sources. This underpopulation may be caused, at least partly, by the omission of previously known optically bright objects from the diagram and by selection effects as objects in this region are radio and X-ray quiet. A substantial fraction of the objects populates the BL Lac region. From these objects candidates for optical follow up programs were selected. They showed a relatively high success rate for being identified as BL Lacs (Laurent-Muehleisen 1996). The majority of objects populate the wide region of quasars. A certain number of objects are found above the dashed line, having unusually low optical flux but with strong radio- and X-ray emission. For most of them only upper limits can be given for the optical magnitudes (open circles). Above the dashed line we find objects with a strongly inverted spectral energy distribution $\alpha_{ro}/\alpha_{ox} > 1$ which might be 'real' optically quiet quasars (Kollgaard et al. 1995) or very red, absorbed radio sources (Webster et al. 1995). Finally, using the VLA flux densities instead of the 87 GB flux densities (which were taken to allow a direct comparison with previously published results) leads to an increase of the dispersion towards lower values of α_{ro}, indicating that the sample contains a non negligible fraction of only moderately beamed objects (see as well L97).

3.5. f_x/f_r versus f_o/f_r

The class separation seen in the $\alpha_{ro} - \alpha_{ox}$ diagram is even more evident when we normalize the fluxes to the radio flux density (all fluxes are converted to units of erg cm$^{-2}s^{-1}$ Hz^{-1}). In Fig. 11 we plot the flux ratios log(f_x/f_r) versus log(f_o/f_r). The open squares represent radio selected BL Lacs (RBL) and highly polarized quasars (HPQ), the open circles X-ray selected BL Lacs (XBL; from Brinkmann et al. 1996b).

The full dots are the objects of our sample which fill in the gap between the above 'extreme' type of objects. They lie near the position of radio-loud quasars (see Fig. 10 of B95 and Fig. 16 of Brinkmann et al. 1996a), shifted diagonally towards higher values of f_x/f_r and f_o/f_r. This appears to be related to the fact that the average radio fluxes are generally about one order of magnitude lower than those of the previously known

Table 6. Results of linear regression analyses

Parameter pair	α	R_{sp}	P_r
$log(R) - m_o$	-0.05	-0.13	0.010
$log(R) - (O - E)$	-0.09	-0.19	0.0002
$\Gamma - m_o$	-0.08	-0.21	$3.0\ 10^{-4}$
$\Gamma - (O - E)$	-0.11	-0.23	$5.6\ 10^{-5}$
$f_o/f_x - f_{core}/f_x$	0.25	0.28	$3.9\ 10^{-9}$
$f_o/f_x - f_{r,tot}/f_x$	0.34	0.29	$1.2\ 10^{-9}$
$\Gamma - f_x$	0.27	0.17	$2\ 10^{-5}$

quasars. However, the corresponding optical and X-ray fluxes should scale roughly similarly. Whether this offset can be purely accounted for by luminosity K-corrections, whether it is caused by unknown selection effects in the current sample or whether it indicates a selection bias towards higher radio fluxes in the previously known objects will only be clear after most of the objects are optically identified.

Further, the class of 'radio-loud' AGN covers a huge range in radio fluxes (fixing the other frequency bands) and this range is not bimodal but rather continuous. This could imply that the previously found gap in the flux ratio diagram was merely caused by selection effects as well and that radio-loud quasars (and, perhaps, BL Lacs) show a nearly linear relation in their flux ratios. Interestingly, only very few objects are found at the extreme flux ratios characteristic for HPQ, radio galaxies, and X-ray selected BL Lacs. As these regions are populated by objects with large radio (HPQ) and optical (galaxies) fluxes most of them are already 'known'. On the other hand, it cannot be ruled out that, for the last two classes, the 'relative' sensitivity of the 87 GB survey might not be sufficient for those objects to be included in the sample. There are very likely many more X-ray selected BL Lacs in the RASS, but with total 5 GHz flux densities below $\sim$ 20 mJy.

3.6. Correlations of X-ray, optical and radio emission

We have further looked for observable correlations between the accessible X-ray, optical, and radio properties but found few statistically significant correlations between source intrinsic physical parameters (correlations between various radio properties of the objects are presented in L97). The results are given in Table 6 where we list the two quantities to be correlated, the slope of the linear correlation, the Spearman rank correlation coefficient, and the probability that no correlation exists.

The radio core dominance parameter[1] $R = f_{core}/f_{lobe}$ is often used as a relative measure of orientation (Orr & Browne 1982). The first four correlations in Table 6 are in accordance with the general picture that the sample contains a certain fraction of galaxies which are optically fainter, redder, and show a flatter X-ray spectrum than quasars. However, the relatively flat slope found for the flux ratio correlations together with the narrow range of the optical - to - X-ray flux ratios indicates that this fraction can not be very large. The correlation between the spectral slope and the X-ray flux seems to be caused by a selection effect as, statistically, objects with the lowest X-ray fluxes tend to have flatter spectra which has been attributed to an increasing contribution of X-ray luminous galaxies (Almaini et al. 1996).

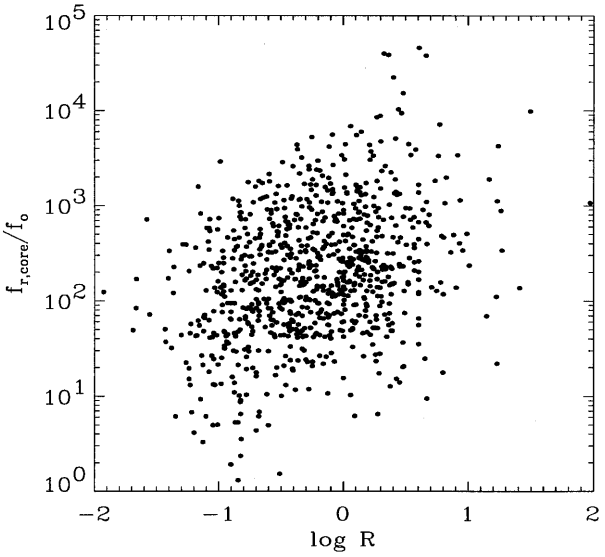

Fig. 12. Correlation between the two orientation parameters: ratio of radio-to-optical flux and core dominance parameter R.

The fact that the flux ratios f_x/f_o and $f_x/f_{r,tot}$ are not strongly dependent on R (P_r = 0.17 and P_r = 0.28, respectively) indicates, that these ratios are either not sensitively dependent on the viewing conditions of the sources or that they scale similarly. For the flux ratio $f_x/f_{r,core}$ there is an inverse trend ($f_x/f_{r,core} \sim -log(R)$) which is discussed in more detail in L97.

It seems as if the sample is relatively homogeneous, and not separable according to its broad band properties without redshift (distance) information and optical classification. This might also be due to the fact that most of the 'extreme' objects like HPQs or XBLL with similar fluxes are already identified previously. Further, more than half of all objects are found in a narrow radio flux interval of $\sim$ 20 - 65 mJy, in contrast to the known objects spanning about three orders of magnitude in radio flux (see Fig. 4a) thus forming a much more 'separable' sample in radio flux space. The only noticeable subgroup is formed by relatively few red objects with very low f_x/f_o ratios (see Fig. 10).

Recently, Wills & Brotherton (1995) have raised some concern on the interpretation of the core dominance R being a good measure for the viewing angle of an object and have instead proposed to use the ratio of core to optical flux as a determining parameter. In Fig. 12 we show a plot of these quantities. There is a statistically significant correlation between these two quantities supporting the idea that both are indicators for the orientation of a source. However, the slope of this correlation

[1] here approximated by the ratio R' = $f_r^{VLA}/(f_r^{GB} - f_r^{VLA})$, see L97

is not unity and the large scatter in the data indicates that at least one of the proposed orientation parameters shows some branching for different object classes. It should be noted, that for the sample of previously known quasars (see Brinkmann et al. 1996a), the scatter in the data is much smaller - but the correlation is probably due to a separation of the objects according to their radio spectral index (steep / flat spectrum quasars).

4. Conclusions

We have presented the broad band properties of a very large sample of 1304 optically unidentified radio-loud X-ray sources from the ROSAT Survey which are in their majority most likely AGN. Combined with the 617 previously identified similar AGN in B95, the RGB is one of the largest well-defined flux-limited surveys of AGN ever obtained.

Most of the new objects have optical magnitudes $m_V \sim 17$-20 which is quite accessible to optical spectroscopy (Fig. 4b). The RGB sample is thus excellent for redshift surveys leading to AGN classification (e.g. quasar vs. BLL), luminosity functions and evolution studies. Note the RGB pushes 1-2 orders of magnitude deeper in both X-ray and radio flux compared to previous unbiased wide-area AGN surveys. Laurent-Muehleisen's thesis, producing the largest well-defined sample of XBLs, is an example of these studies.

The X-ray spectra (Figs. 5-6) and broad-band colors (Fig. 9) as well as various correlations of the source properties indicate that most of the unidentified RGB sources are new quasars, although some XBLs, radio galaxies, Seyferts and clusters are undoubtably present. However, there are some subtle differences in their properties compared to those of known radio-loud quasars which might indicate selection biases in either of the samples or bulk properties slightly different from those inferred from the very radio bright end of the distribution. The optical identification of a large number of the objects is required to obtain a better understanding of the properties of the class of radio-loud quasars.

The majority of the new RGB sources have broad-band properties between those of traditional radio-selected and X-ray selected AGN (Fig. 11). There is no bimodal distribution in the radio-loudness distribution, and it is quite possible that the distribution extends smoothly into the radio-quiet regime. The traditional division between radio-quiet and radio-loud AGN may not be warranted. X-ray surveys may thus be uncovering a missing AGN population with radio properties intermediate between the traditional radio-loud AGN (PKS and 1Jy samples) and radio-quiet AGN.

Acknowledgements. We thank the referee, Rogier Windhorst, for helpful and constructive comments. The ROSAT project is supported by the Bundesministerium für Bildung, Wissenschaft, Forschung und Technologie (BMBF) and the Max-Planck-Gesellschaft. We thank our colleagues from the ROSAT group for their support. At Penn State, this work was supported by NASA grant NAGW-2120. This research has made use of the NASA/IPAC Extragalactic Data Base (NED) which is operated by the Jet Propulsion Laboratory, California Institute of Technology, under contract with the National Aeronautics and Space Administration.

References

Almaini O., Shanks T., Boyle B.J., et al., 1996, MNRAS in press
Brinkmann W., Siebert, J., Boller, Th., 1994, A&A 281, 355
Brinkmann W., Siebert J., Reich W., et al., 1995, A&AS 109, 147 (B95)
Brinkmann W., Yuan W., Siebert J., 1996a, A&A in press
Brinkmann W., Siebert J., Kollgaard R.I., Thomas H.-C., 1996b, A&A 313, 356
Cappi M., Matsuoka M., Comastri A., et al., 1997, to appear in ApJ 478 (April 1, 1997)
Condon J.J., Broderick J.J., Seielstad G.A., 1989, AJ 97, 1064
Dickey J.M., Lockman F.J., 1990, ARA&A 28, 215
Draper N.R., Smith, H., Applied Regression Analysis, John Wiley, New York, 1966
Hook I.M., McMahon R.G., Irvin M.J., Hazard C., 1996, MNRAS 282, 1274
Kock A., Meisenheimer K., Fürst E., et al., 1996, A&A 307,745
Kollgaard R.I., Feigelson E.D., Laurent-Muehleisen S.A., et al., 1995, ApJ 449, 61
Kühr H., Nauber U., Pauliny-Toth I.I.K., Witzel A., 1979, MPIfR preprint No. 55
Laurent-Muehleisen S.A., 1996, PhD thesis, Penn State University
Laurent-Muehleisen S.A., Kollgaard R.I., Ryan P.J., et al., 1997, A&AS in press (L97)
Law-Green J.D.B., Leahy J.P., Alexander P., et al., 1995, MNRAS 274, 939P
Maccacaro T., Gioia I. M., Wolter A., Zamorani G., Stocke J., 1988, ApJ 326, 680
McMahon R.G., 1991, in: The Space Distribution of Quasars, Ed. D. Crampton, ASP Conference Series, Vol 21, p. 129
Marcha M.J.M., Browne I.W.A., Impey C.D., Smith P.S., 1996, MNRAS 281, 425
Nass P., Bade N., Kollgaard R.I., et al., 1996, A&A 309, 419
Neumann M., Reich W., Fürst E., et al., 1994, A&AS 106, 303
Orr M.J.L., Browne I.W.A., 1982, MNRAS 200, 1067
Perlman E., Stocke J.T., Schachter J., et al., 1996, ApJS 104, 251
Schartel N., 1995, PhD thesis, University of München
Stark A.A., Gammie C.F., Wilson R.W., 1992, ApJS 79, 77
Stickel M., Kühr H., 1996, A&AS 115, 11
Stocke J.T., Morris S.L., Gioia I.M., et al., 1991, ApJS 76, 813
Tananbaum H., Avni Y., Branduardi G., et al., 1979, ApJ 234, L9
Trümper J., 1983, Adv. Space Res. Vol. 2, No. 4, 241
Vikhlinin A., Forman W., Jones C., Murray S., 1995, ApJ 451, 564
Voges W., 1992, In: Proc. of the ISY Conference "Space Science", ESA ISY-3, ESA Publications, p.9
Voges W., Gruber R., Paul J., et al., 1992, In: Proc. of the ISY Conference "Space Science", ESA ISY-3, ESA Publications, p.223
Wall J., 1996, invited talk at the IAU Symposium 179 "New Horizons from Multi-Wavelegth Sky Surveys", Baltimore.
Wagner S., 1996, talk given at the IAU Symposium 179 "New Horizons from Multi-Wavelegth Sky Surveys", Baltimore.
Webster R.L., Francis P.J., Peterson B.A., Drinkwater M.J., Masci F.J., 1995, Nature 375, 469
Wills B.J., Brotherton M.S., 1995, ApJ 448, L81
Windhorst R.A., Kron R.G., Koo D.C., 1984, A&AS 58, 39
Worral D.M., Wilkes B.J., 1990, ApJ 360, 396

This article was processed by the author using Springer-Verlag LaTeX A&A style file *L-AA* version 3.